

# The Role of Network Topology on the Initial Growth Rate of Influenza Epidemics

*J. Hyman* <sup>\*</sup>, *S. Khatri* <sup>†</sup>, *R. Rael* <sup>‡</sup>  
 Los Alamos National Laboratory  
 T-7 and Center for Nonlinear Studies  
 Los Alamos, New Mexico

August 8, 2003

## Abstract

We use networks, powerful abstract representations of systems of interacting elements, to represent multiple interacting populations and explore the effects of the topologies on the initial growth rate of influenza epidemics. Graph theory applied to epidemiological models may yield insight into the nature of disease dynamics and provide important complementary perspective on understanding these models. We analyze the basic SIR model on three general networks: ring, square lattice, small world networks. We explore the evolution of the dominant eigenvalues as the network size increases for two different cases, when the total population remains constant and when the total population increases as the network size increases. The analysis is carried out via numerical simulations as well as through the mathematical analysis of simple cases.

---

<sup>\*</sup>T-7, LANL

<sup>†</sup>New York University

<sup>‡</sup>University of Arizona

# 1 Introduction

Mathematical models in epidemiology have become vitally important in the development of disease prevention strategies. As human populations grow and the far corners of the world are more closely linked to one another with transportation such as airlines it is now feasible for infectious disease to spread rapidly across continents, as seen recently with the outbreak of SARS. Networks provide a way to model more complex dynamics of the spread of infectious disease over large scale areas. Unfortunately, realistic graphical representations of large-scale systems such as urban environments are computationally and analytically unmanageable.

Network models of the spread of disease allow for high levels of complexity in interactions to be taken into account. These models may aid the scientific and medical communities in addressing these issues by providing them with an effective understanding of the growth and propagation of disease, thus elucidating approaches toward the prevention of destructive wide-spread epidemics. Advanced epidemiological models, particularly the agent-based decision support simulation system EpiSims, are providing insight into the nature of disease dynamics with fine scale resolution. Concurrently, modern network theory is providing important perspective on understanding the nature of the properties of these graphical models.

A method of reducing the magnitude of such networks would contribute to increasing the efficiency of computation of complex disease dynamic models. However, there is great underlying complexity in the derivation of such a method involving the preservation of various properties of the original network. Because of the inevitability of information loss in network reduction, a first major issue to resolve in approaching this problem is to determine which properties to preserve. A basic understanding of the effects of dynamic interactions on epidemic propagation is an important step in the direction of reducing the magnitude of large-scale networks.

Using an influenza epidemic model, an SIR model with no disease-induced death, we look for an understanding of the initial growth rate on networks ranging in complexity. We study the evolution of the dominant eigenvalues of the linearized system as the network size increases in a ring, square lattice, and small world network. Also, we observe the distribution of the eigenvalues as the network size increases.

Influenza is a disease which has been around for many years and even today it occurs annually around the world. Even with our advanced technology we are yet not capable of fully understanding the spread of an epidemic. Influenza spreads between social groups through just a few contacts. Within these social groups, the disease spreads rapidly. By looking at mathematical models, we gain information on how the disease spreads between groups and what can be done to prevent this spread.

With information about how influenza spreads, preventative measures can be taken. Influenza is a disease which kills numerous people every year. These lives can be saved if we have a better understanding of how the disease spreads within the population. With this information we would be able to better prevent high risk populations from being exposed to the infection. Also with this knowledge, decision

makers can help reduce influenza spread through the production of vaccines and other preventative measures.

By increasing knowledge of the initial rate of infection, we hope to contribute to the future possibility of allowing for the approximation of a network on the scale of urban disease spread by a much smaller model amenable to evaluation by the scientific and medical communities.

## 2 Overview

After years of being considered a problem of the past, infectious diseases have once again been recognized as an urgent public health problem. It has become important to use all of the tools available to devise effective strategies to minimize the impact and spread of infectious diseases, and to predict and understand the development and spread of resistant strains. Epidemic models of the spread of a disease through a population can help the medical/scientific community anticipate the course of an epidemic, discern the factors driving its growth, and evaluate the potential effectiveness of different approaches for bringing an epidemic under control.

The general framework that we propose will be suitable for epidemiological investigation of any contagious disease outbreak. We will apply our model to influenza, in particular, with indications of its application to smallpox, because smallpox remains a disease of great concern, with the potential to kill large numbers of individuals.

We will model the spread of an epidemic generally using coupled differential equations describing the fraction of a population in any of a small number of states (e.g. susceptible, infected) as a function of time. The biology of an infectious disease is complex and, therefore, so must be the model if it is to be used for quantitative predictions. Key biological parameters for modeling an infectious epidemic include:

- *Transmission* - the ability of individuals to expose others to the infection.
- *Susceptibility* - the sum of biological mechanisms that reduce an individual's protection against infection.
- *Recovery* - the rate at which a recovered individual retains some level of immunity to infection.

The coupled rate equations for the spread of an epidemic are appropriate when considering a small number of parameters, large populations, and outbreaks in populations with only modest heterogeneity in the social behavior of the susceptible population within a particular location. They average over the details of how disease spreads from person to person, assuming in effect that the whole population is well mixed. They can only crudely distinguish the epidemiological consequences of a disease's properties (susceptibility, latency, etc.) from those produced by the structure of social interactions (many small isolated groups, a few individuals who interact with

many others, etc.). Thus they shed only a dim light on how to target sub-populations for intervention strategies.

Some attempts have been made to connect different locations by a mobility/transportation network. For example, Rvachev and Longini partition a region's population by city and estimate the transmission rate among cities based on the number of travelers [10]. The small-world models introduced by Watts and Strogatz demonstrate the richness of dynamics that can be produced by introducing a small number of partitions [14].

The mixing of the population, which allows the virus to spread from person to person, is a complex social phenomenon, varying across cultures and between individuals, and over the life history of a given individual. The distribution of social mixing within a population and the amount of mixing between behavioral levels has been found to be an important determinant of the rate and extent of spread of many infectious diseases.

### 3 Epidemic Models on Networks

Many traditional epidemiological models implicitly contain the assumption of homogeneous mixing which means that all individuals in a population contact each other with equal probability. While this condition may be relevant within small populations, it is not likely to hold for large populations such as those of cities. We take the approach of applying an SIR model onto a network to allow for heterogeneous mixing between groups.

A network is a mathematical structure consisting of nodes (or vertices) and edges connecting these nodes. In applying networks to epidemic models, the nodes may represent people or groups of people. People may be grouped demographically such as by age class, race or socioeconomic group, or geographically at many levels such as by building, neighborhood, or city. Edges may be directed or undirected and represent connections between groups such as number of contacts, rate of contact, visitation, or migration.

Careful consideration must be given to the structure of the network used to model interactions. The mass-action law "seriously affects the qualitative and quantitative behavior of models with interacting subpopulations of varying size" [4]. What this means in an epidemic model on interacting populations, is that the total number of contacts between group A and group B must be equal to the total number of contacts between group B and group A. If the total populations in groups A and B are constant and equal, this implies that there is no net inflow or outflow of people. This may be the case when nodes represent static demographic groups, that is, when individuals do not move from group to group. In this case, an edge may be undirected and represent rate of contact  $c_{ij}$  between groups  $i$  and  $j$ . Since the total populations are equal  $N_A = N_B$ , then the total number of contacts is preserved  $N_A c_{ij} = N_B c_{ji}$  (Figure 1). This same undirected graph may represent visitation, in which case nodes represent locations from which people leave and contact people from an adjacent group, but ultimately return to their original location.

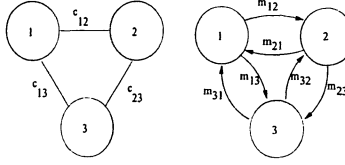


Figure 1: *Examples of a contact (undirected) graph and a mobility (directed) graph.*

In contrast, directed graphs are used to represent the number of people travelling from one location to another,  $m_{ij}$ , in which case, conservation of contact number does not play a role (??).

For simplicity, we use undirected graphs representing contact between groups of constant and equal size. We apply an epidemic model on this structure to allow for heterogeneous mixing and analyze its dynamics.

## 4 SIR Model

### 4.1 Simple SIR Model

The epidemiological model known as the SIR model is one in which the population consists of three classes of individuals: those who are susceptible to a disease, those who are infected and infectious, and those who have recovered (Figure 2). Thus, the disease persists throughout the duration of the time period considered. With no disease-related death, this model is applicable to diseases such as influenza when working over short periods of time, where the population does not lose their immunity to the disease.

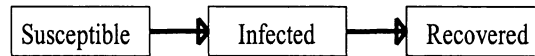


Figure 2: *The way an epidemic spreads in a simple SIR model.*

In 1927, Kermack and McKendrick created the simple SIR model [8]. This model assumes a homogeneous population with random mixing. This model is given by the following set of equations:

$$\dot{S} = -\lambda S \quad (1)$$

$$\dot{I} = \lambda S - \alpha I \quad (2)$$

$$\dot{R} = \alpha I, \quad (3)$$

where  $\lambda$  represents the rate of infection and  $\alpha$  is the rate at which infected people recover. The rate of infection is defined as the product of the rate of contact (number

of contacts per time)  $r$ , the transmissibility of the disease (probability of infection per contact given the contact is infected)  $\beta$ , and the proportion of infected individuals  $\frac{I}{N}$ :

$$\lambda = r\beta \left( \frac{I}{N} \right). \quad (4)$$

## 4.2 Migration Terms

Migration terms are added to represent the people leaving and entering the system. An equal proportion,  $\mu$ , of the susceptible, infected, and recovered people leave the system but only susceptible people enter the system. Including these terms the system is:

$$\dot{S} = -\lambda S + \mu(\Lambda - S) \quad (5)$$

$$\dot{I} = \lambda S - \alpha I - \mu I \quad (6)$$

$$\dot{R} = \alpha I - \mu R. \quad (7)$$

Assuming the population has stabilized allows us to set those entering the system equal to those leaving. Hence, without loss of generality it can be assumed that

$$\Lambda = S + I + R = N. \quad (8)$$

## 5 Networks

We have analyzed and observed the initial growth rate of this SIR model, using parameters from influenza data, on three different networks: ring, square lattice, and small world networks.

### 5.1 Ring Networks

Applying the SIR model to a ring network generalizes the simple SIR model by dividing the population into  $n$  groups — or small worlds — based on age, socio-economic status or other factors (e.g. the black circles in Figure 3) [12, 11]. People mainly interact with members of their own group. The model also allows for interactions with neighboring groups — such as the age groups right above or below a person's own age group (e.g. the outer circle in Figure 3).

Each group,  $i$ , is modeled as in refbasicSIR yielding a  $3n$  dimensional system:

$$\dot{S}_i = -\lambda_i S_i + \mu(N_i - S_i) \quad (9)$$

$$\dot{I}_i = \lambda_i S_i - \alpha I_i - \mu I_i \quad (10)$$

$$\dot{R}_i = \alpha I_i - \mu R_i. \quad (11)$$

The parameter,  $\lambda_i$  is dependent on the percent of infected people within the group and also on the percent in the neighboring groups:

$$\lambda_i = \beta r \left[ \theta_{i,i+1} \left( \frac{I_{i+1}}{N_{i+1}} \right) + \theta_{i,i} \left( \frac{I_i}{N_i} \right) + \theta_{i,i-1} \left( \frac{I_{i-1}}{N_{i-1}} \right) \right], \quad (12)$$

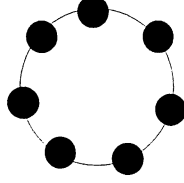


Figure 3: *A representation of a ring network and how people interact with others within the population.*

where  $\theta_{i,i}$  is the proportion interactions that members of group  $i$  have with people of their own group,  $\theta_{i,i+1}$  is the proportion of interactions a person in group  $i$  has with the people in it's neighboring group  $i + 1$ , and  $\theta_{i,i-1}$  is proportion of interactions a person in group  $i$  has with people in group  $i - 1$ . Since  $\theta$  values are all proportions,

$$\sum_{j=1}^n \theta_{i,j} = 1 \quad (13)$$

We are assuming uniformity in the the proportion of contacts group  $i$  has with it's two neighbors by letting  $\theta_{i,i-1} = \theta_{i,i+1} = \frac{(1-\theta_{i,i})}{2}$ . Therefore, when the local population in each node is equal, the contacts a group  $i$  has with other groups is equally split between these two neighboring groups.

## 5.2 Interactions between Groups

Not only must the sum of the proportion of interactions each group has be equal to one, but also the number of contacts group  $i$  has with group  $j$  must be equal to the number of contacts group  $j$  has with group  $i$ . So, each  $\theta_{i,j}$  and  $\theta_{j,i}$  must satisfy,

$$r\theta_{i,j}N_i = r\theta_{j,i}N_j. \quad (14)$$

This is accomplished by all of the models presented here because the local population in every node is equal, and each  $\theta_{i,j} = \theta_{j,i}$ .

## 5.3 Square Lattice Networks

After observing the spread of SIR epidemics on a ring network, we can consider more complex interactions between the groups by using a two dimensional periodic  $n \times n$  lattice to model the population (Figure 4).

The system of equations for each node remains the same but now has slightly different notation, for each node  $(i, j)$ ,

$$\dot{S}_{i,j} = -\lambda_{i,j}S_{i,j} + \mu(N_{i,j} - S_{i,j}) \quad (15)$$

$$\dot{I}_{i,j} = \lambda_{i,j}S_{i,j} - \alpha I_{i,j} - \mu I_{i,j} \quad (16)$$

$$\dot{R}_{i,j} = \alpha I_{i,j} - \mu R_{i,j}. \quad (17)$$

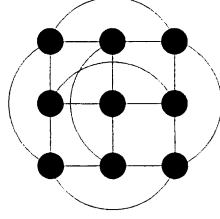


Figure 4: A representation of a periodic  $3 \times 3$  square lattice network and how people interact with others within the population.

In this system of equations,  $\lambda$  is now dependent on the infected population in the four neighbors of node  $(i, j)$ . At the internal nodes,

$$\lambda_{i,j} = \beta r \left[ \theta_{i,j+1}^{i,j} \left( \frac{I_{i,j+1}}{N_{i,j+1}} \right) + \theta_{i+1,j}^{i,j} \left( \frac{I_{i+1,j}}{N_{i+1,j}} \right) + \theta_{i,j}^{i,j} \left( \frac{I_{i,j}}{N_{i,j}} \right) \right. \quad (18)$$

$$\left. + \theta_{i,j-1}^{i,j} \left( \frac{I_{i,j-1}}{N_{i,j-1}} \right) + \theta_{i-1,j}^{i,j} \left( \frac{I_{i-1,j}}{N_{i-1,j}} \right) \right] \quad (19)$$

At the borders, we can use the same equation for  $\lambda_{i,j}$  as in equation (18) but if  $i-1=0$  or  $j-1=0$  then  $0 \rightarrow n$ , and if  $i+1=n+1$  or  $j+1=n+1$  then  $n+1 \rightarrow 1$ . In these equations,  $\theta_{s,t}^{i,j}$  is the proportion of contacts group  $(i, j)$  has with group  $(s, t)$ . Here, as in the ring network,

$$\sum_{t=1}^n \sum_{s=1}^n \theta_{s,t}^{i,j} = 1 \quad (20)$$

Once again, we assume uniformity in the proportion of contacts groups have by letting  $\theta_{i+1,j}^{i,j} = \theta_{i,j+1}^{i,j} = \theta_{i-1,j}^{i,j} = \theta_{i,j-1}^{i,j} = \frac{(1-\theta_{i,j}^{i,j})}{4}$ . Therefore,  $\theta_{i,j}^{i,j}$  is the proportion of contacts members of group  $(i, j)$  have with members within their own group and  $\frac{1-\theta_{i,j}^{i,j}}{4}$  is the proportion of contacts members of group  $(i, j)$  have with members of each of their four closest neighboring groups.

## 5.4 Small World Ring Networks

Watts and Strogatz define a small world model as a ring network where each node is connected to  $r$  neighbors initially, and then each edge is removed with probability  $p$  and reconnected to another node in the network randomly (Figure 5) [14]. In our model we let  $r$  equal one, so we are beginning with the ring network described above (Figure 3). The edges which are removed between neighbors and then reconnected with other random nodes represent random interactions between distant groups — such as people meeting on a subway. The system of equations remains the same but  $\lambda$  changes, so that it allows for each group to have interactions with all the other



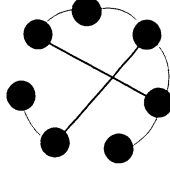


Figure 5: A representation of a small world ring network model where the radius of the network,  $k$  is 1 and the parameter  $p$  is the probability that an edge will be disconnected in the ring and then randomly reconnected.

groups in the model,

$$\lambda_i = \beta r \left[ \theta_{i,1} \left( \frac{I_1}{N_1} \right) + \theta_{i,2} \left( \frac{I_2}{N_2} \right) \dots \theta_{i,i} \left( \frac{I_i}{N_i} \right) + \theta_{i,i+1} \left( \frac{I_{i+1}}{N_{i+1}} \right) \dots \theta_{i,n} \left( \frac{I_n}{N_n} \right) \right]. \quad (21)$$

Here, the constant,  $\theta_{i,j}$ , is the proportion of interactions people in group  $i$  have with people in group  $j$ , and  $I_j/N_j$  is the proportion of people in group  $j$  who are infected. Since each  $\theta_{i,j}$  is a proportion,

$$\sum_{j=1}^n \theta_{i,j} = 1 \quad (22)$$

## 6 Parameters

The parameters used in these models are presented in Table 1. These values allow us to model the spread of influenza over short periods of time. Acceptable ranges for parameters were given by Hyman and Laforce [7]. The ranges for most of the parameters were found in epidemiological papers [1, 13]. Hyman and Laforce chose values for the number of adequate contacts (probability of transmitting the infection) per unit time,  $r\beta$ , by conducting least squares analysis on a multi-city model.

Meaning	Parameter	Baseline
rate of recovery (1/days) [1]	$\alpha$	0.2439
number of adequate contacts per unit time (contacts/day)	$r\beta$	0.246
removal rate of people from population in the absence of infection(1/days)	$\mu$	0.0002740

Table 1: This table shows all the influenza parameter values used in the model and all the simulations presented in this paper. These values were taken from Hyman and Laforce [7].

## 7 Initial Growth Rate Analysis

For a system of  $n$  nodes in all of the networks, we analyze the initial growth rate by linearizing the system near the disease free equilibrium point (when time = 0). First, we simplify the system by keeping each  $N_i$  constant. This is a valid assumption since influenza occurs over a short period of time and also because we are only looking at the spread of the disease initially. Therefore, we can reduce the system in each node to:

$$\dot{S}_i = -\beta r \sum_{j=1}^n \theta_{i,j} \frac{I_j}{N_j} S_i + \mu(N_i - S_i) \quad (23)$$

$$\dot{I}_i = \beta r \sum_{j=1}^n \theta_{i,j} \frac{I_j}{N_j} S_i - \alpha I_i - \mu I_i. \quad (24)$$

Then, we can solve for  $R_i$ ,

$$R_i = N_i - S_i - I_i. \quad (25)$$

### 7.1 Linearization

As explained in Appendix 1, we linearize the system of differential equations for  $n$  nodes near the disease free equilibrium point. Since we are interested in the initial growth rate of the disease we look only at the infected class of each node at  $t = 0$ . So we have a system of  $n$  equations to linearize,

$$\dot{I}_i = \beta r \sum_{j=1}^n \theta_{i,j} \frac{I_j}{N_j} S_i - \alpha I_i - \mu I_i. \quad (26)$$

The Jacobian of this system is

$$\begin{bmatrix} -\mu - \alpha + \beta r \theta_{1,1} & \beta r \theta_{1,2} & \dots & \beta r \theta_{1,n} \\ \beta r \theta_{2,1} & -\mu - \alpha + \beta r \theta_{2,2} & \dots & \beta r \theta_{2,n} \\ \vdots & \ddots & & \vdots \\ \vdots & & \ddots & \vdots \\ \beta r \theta_{n,1} & \dots & & -\mu - \alpha + \beta r \theta_{n,n} \end{bmatrix}. \quad (27)$$

The role of the Jacobian in initial growth rates and stability can be found in the appendix. By computing the eigenvalues of the Jacobian matrix, we are able to understand when the infected population of the network increases and leads to an epidemic of influenza (when the dominant eigenvalue is greater than zero) and when the disease dies out (when the dominant eigenvalue is less than zero). We analyzed what was happening as we added nodes to each network. By adding a node to the network, we are adding another equation to the system. Then we observe the dominant eigenvalues of the different systems to try to understand the effect of adding nodes on the spread of the disease.

## 7.2 Numerical Analysis

Using Matlab, we numerically calculated the eigenvalues of the Jacobian presented above for all three types of networks as the number of nodes in the network increased. We did this by using an ordinary differential equation solver (ODE113 in Matlab) to solve the system of equations using the appropriate  $\theta$  matrix depending on the network for a short amount of time (around ten days). Then, we used the equations for the elements of the Jacobian at time equal to zero and then solved for the eigenvalues.

For all three networks, we varied the initial conditions while maintaining equal populations in all  $N_i$ . First, one hundred people were allocated to each node, even as the number of nodes increased, therefore as the network grew the population grew. In the other two cases of initial conditions, we maintained the entire population at 5,000 and 10,000 respectively, and divided the population equally by the number of nodes present in the network. In all cases the disease was spread by one person in one group.

The only parameter we varied and observed the effects of was  $\theta$ . For each initial condition in each network, we set every  $\theta_{i,i}$ , the proportion of contacts group  $i$  has with members of their own group, equal to 0.25, 0.50, 0.75, and 1.0. Then the remaining contacts were equally split among all the other groups that this group  $i$  was connected to depending upon the network.

### 7.2.1 Numerical Results: Ring and Square Lattice Networks

As would be expected for all types of networks, when  $\theta_{i,i} = 1$  the dominant eigenvalue is just equal to the dominant eigenvalue as if the one node the infected person initially resides in is the entire population. This value is 0.002054 with the influenza parameters, therefore an influenza epidemic takes off in the one node with the infected person but the infection does not spread to the rest of the population.

For all the other values of  $\theta_{i,i}$ , since the local populations in each node were equal and the contacts with other groups were equally divided, the disease spread as if the entire population was in one node (homogeneous mixing). This result did not vary with the different initial conditions. Once again, this means that the dominant eigenvalue was equal to 0.002054 as in the case where  $\theta_{i,i} = 1$ .

Since the lattice network is just an expansion of the ring network in the sense that each node is connected to the four closest neighbors rather than just the two closest, the same results were observed for both the square lattice and ring networks, as expected

### 7.2.2 Numerical Results: Small World Network

First, we observed cases with the small world network where  $p$ , the probability an edge would be disconnected from a neighbor and randomly reconnected to another node, was set equal to 0.1. Since each small world network is formed based on some randomness, having the same initial conditions and parameters does not guarantee the

same network. Therefore, when trying to find the dominant eigenvalues of different sized networks, we took the average of the dominant eigenvalue of fifty networks with the number of nodes, the parameters, and the initial conditions we wanted. These results can be seen in figure 6 for one initial condition. The blue pluses show the dominant eigenvalues of each of the fifty networks, and the red plus shows the mean. We observed that as the number of nodes increased the dominant eigenvalues generally increased. Also, as the proportion of interactions members of a group had outside of their respective group, the dominant eigenvalue increased slightly. Similar results were seen with the other two initial conditions.

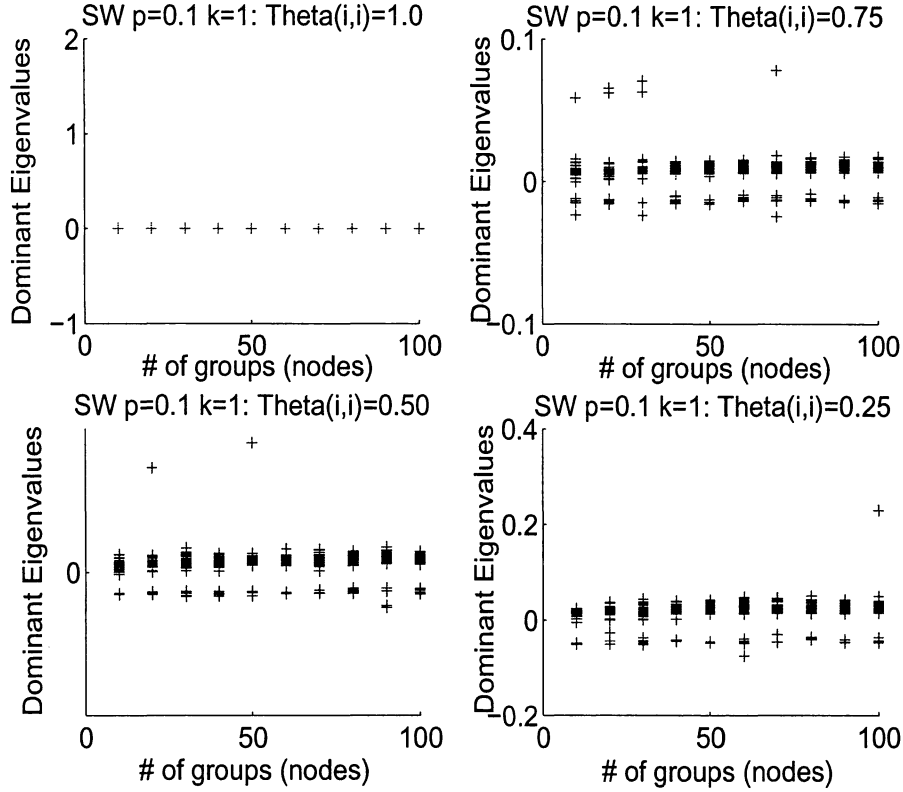


Figure 6: *Small World Network: The total population of all the nodes always equal 5000 people. As the number of nodes increases the mean dominant eigenvalue increases and as the proportion of contacts outside one's own group decreases, the mean dominant eigenvalue increases.*

After varying the number of nodes, we decided to fix the number of nodes at one hundred and look at what happens to the eigenvalues when we vary  $p$ . We observed the largest and the second largest eigenvalues as  $p$  varied between zero and one (Figures 7 and 8). Once again we ran fifty realizations at each  $p$  value since the building of a small world network is a stochastic process.

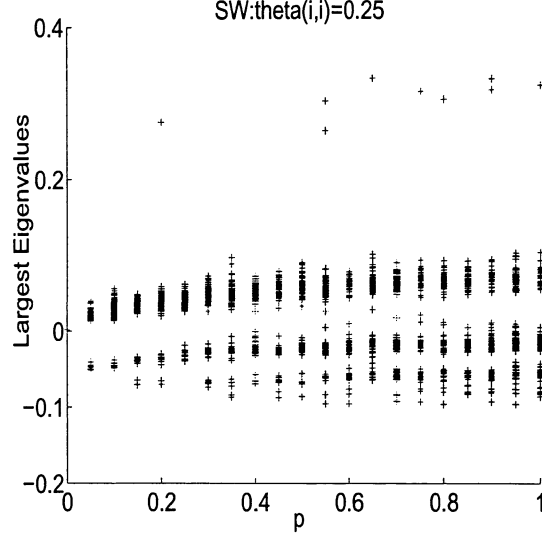


Figure 7: *Small World Network: We set the number of nodes equal to 100 (with each node having exactly one hundred people) as we varied  $p$  and observed the largest eigenvalue. Notice when  $p$  is less than 0.5 the mean dominant eigenvalues increase but then after  $p = 0.5$  level off. Also, when  $p$  is greater than 0.5, there is are epidemics taking off more quickly even though the mean is lower.*

We also observed all one hundred eigenvalues for  $p = 0$ ,  $p = 0.1$ , and  $p = 1$  (Figure 9).

These plots showed us that while  $p$  was less than 0.5, as  $p$  increased the largest and second largest eigenvalues increased. Once  $p$  was greater than 0.5, the largest and second largest eigenvalues leveled off (and even possibly decreased). Once again, all three initial conditions resulted in similar data.

### 7.3 Analytic Solution: A Ring Case

We first attempted to solve for the eigenvalues of the Jacobian for all three networks numerically. Looking more closely, we see that we can solve for the eigenvalues of the ring network analytically when considering the case where every  $\theta_{i,i}$  is equal to  $\theta$  and

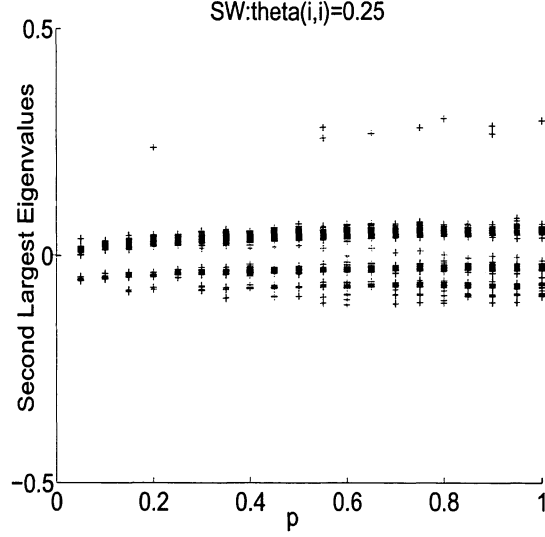


Figure 8: emSmall World Network: We set the number of nodes equal to 100 (with each node having exactly one hundred people) as we varied  $p$  and observed the second largest eigenvalue. The second largest eigenvalues follow the exact same pattern as the largest eigenvalues.

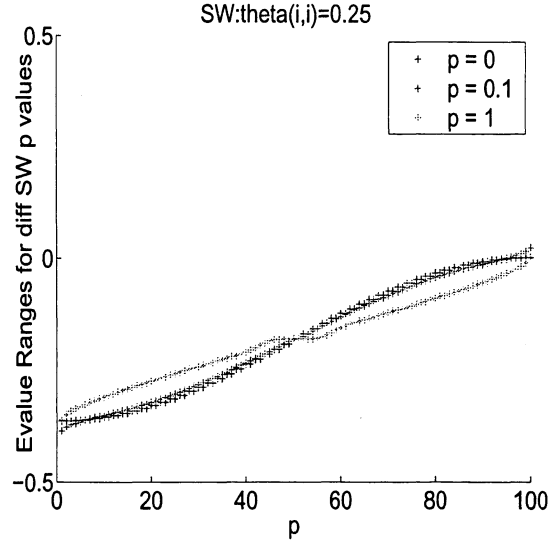


Figure 9: *Small World Network*: We set the number of nodes equal to 100 (with each node having exactly one hundred people) as we observed all the eigenvalue when  $p = 0$ ,  $p = 0.1$ , and  $p = 1$ . The plots for  $p = 0$  and  $p = 0.1$  are similar, while the one for  $p = 1$  has a different shape with a flat region in the middle.

each  $\theta_{i,j} = \frac{1-\theta}{2}$  where  $i \neq j$ . The Jacobian for this ring network is

$$\begin{bmatrix} -\mu - \alpha + \beta r \theta & \beta r \frac{1-\theta}{2} & 0 & \dots & 0 & \beta r \frac{1-\theta}{2} \\ \beta r \frac{1-\theta}{2} & -\mu - \alpha + \beta r \theta & \beta r \frac{1-\theta}{2} & 0 & \dots & 0 \\ 0 & \ddots & \ddots & \ddots & 0 & 0 \\ \vdots & & \ddots & \ddots & \ddots & \vdots \\ 0 & 0 & \dots & \beta r \frac{1-\theta}{2} & -\mu - \alpha + \beta r \theta & \beta r \frac{1-\theta}{2} \\ \beta r \frac{1-\theta}{2} & 0 & \dots & 0 & \beta r \frac{1-\theta}{2} & -\mu - \alpha + \beta r \theta \end{bmatrix}. \quad (28)$$

The eigenvectors of this matrix are

$$\begin{bmatrix} e^{-\frac{ik(n-1)}{2}} \\ e^{-\frac{ik(n-3)}{2}} \\ \vdots \\ e^0 \\ \vdots \\ e^{\frac{ik(n-3)}{2}} \\ e^{\frac{ik(n-1)}{2}} \end{bmatrix}, \quad (29)$$

and the corresponding eigenvalues to be  $\lambda = -\mu - \alpha + \beta r + \beta r \theta (1 - \cos k)$  [5]. We can show that the dominant eigenvalue occurs when  $k = 0$  and therefore the eigenvalue is  $\lambda = -\mu - \alpha + \beta r$  and the corresponding eigenvector is  $[111 \dots 11]^T$ .

Using the Gerschgorin's theorem, we know that any eigenvalue,  $\lambda_i$  of this Jacobian, must satisfy the condition,

$$|-\mu - \alpha + \beta r \theta - \lambda| \leq \left| \beta r \frac{1-\theta}{2} \right| + \left| \beta r \frac{1-\theta}{2} \right|. \quad (30)$$

Therefore, any eigenvalue of this Jacobian is bounded by  $-\mu - \alpha + \beta r$ , so  $\lambda = -\mu - \alpha + \beta r$  must be the dominant eigenvalue [9].

## 8 Conclusions

For the cases we looked at with the ring and square lattice networks there are not critical local populations at which the disease will die out. But in these cases we assumed the local populations were all the same size and that the contacts members of a group had with members of other groups were equal, but this is not the case in the real world. The world is much more like the small world networks used here. In these we can see that how the population is divided does make a difference in if the influenza epidemic takes off or not. We observed that as the number of nodes increased the epidemic took off a little more quickly. Similar results were seen when the proportion of contacts a group had outside of itself increased.

For the small world model, we also decided to fix the number of groups the population was divided into and observe what happens as  $p$ , the probability that an edge is removed and then randomly reconnected, was varied. When  $p = 0$ , the network is equivalent to a ring network, and when  $p = 1$ , the network is completely random. We observed as  $p$  increased until 0.5, as the network changed from a ring network to a more random one, the largest eigenvalue increased but after  $p = 0.5$ , the largest eigenvalue leveled off. This is due to the fact that while  $p$  is less than 0.5, the diagonal of the Jacobian is dominant but this is not the case after that.

By studying the initial growth rates through dominant eigenvalues (and largest eigenvalues) of the SIR model on different networks we can better understand the impact of our society's organization on the spread of diseases. Understanding this allows us to know what kind of reorganization would be useful in preventing the initial spread of a newly introduced disease.

## 9 Future Work

This paper presents just the beginning of the work that can be done on looking at initial growth rates of epidemics on different networks. This work can be continued by looking for the local critical population in small world networks with any parameters and initial conditions and for lattice and ring networks when the local population and number of contacts are not equal for every group. Also, these ideas can be expanded to include scale free networks and the initial growth rate on those networks. Not only should we be looking at the dominant eigenvalue but also the range of all of the eigenvalues as the number of nodes increases in the networks.

In this paper we are looking at the relationship between eigenvalues and initial growth rate. We can take this one step further by seeing how the eigenvalues of the linearized system at nonequilibrium points changes as the epidemic progresses.

## 10 Acknowledgments

We would like to acknowledge and thank Leon Arriola, Carlos Castillo-Chavez, Nakul Chitnis, Gerardo Chowell-Puente, Jia Li, Juan Restrepo, Baojun Song, and Abdul-Aziz Yakubu for all their assistance, knowledge, time, and patience.

The process of working on this project has allowed me to learn not only the mathematical and computational skills involved but also the process of producing a model and working through the scientific procedure. There are no guarantees of getting great results (or any results) the first path one chooses when conducting research. I have learned so much through the task of choosing what path to try next and dealing with the frustrations and joy of gaining results not expected. As a student getting ready to enter graduate school, I appreciate the experience of planning and working through my own project and am grateful to all of those who have made this possible.



Shilpa Khatri

## References

- [1] Addy, C. L., I. M. Longini, and M. Haber, *A generalized stochastic-model for the analysis of infectious-disease final size data*, Biometrics, 47(3):961-974, 1991.
- [2] Brauer, Fred, *A Model for an SI Disease in an age-structured population*, Discrete Contin. Dyn. Syst.-Ser. B 2(2):257-264, May 2002.
- [3] Castillo-Chavez, Carlos, Fred Brauer, *Mathematical Models in Population Biology and Epidemiology*, Springer-Verlag New York Inc.: New York, 2001.
- [4] Castillo-Chavez, Carlos, Jorge X. Velasco-Hernandez, and Samuel Fridman, *Modeling contact structures in biology*, Frontiers of Mathematical Biology, Lecture Notes in Biomathematics 100:454-91, 1994.
- [5] Gustafsson, Bertil, Heinz-Otto Kreiss, and Joesph Oliger, *Time Dependent Problems and Difference Methods*, John Wiley & Sons Inc.:New York, USA, 1995, pp. 17-19.
- [6] Hethcote, Herbert W., *The Mathematics of Infectious Diseases*, SIAM Review, 42(4):599-653, 2000.
- [7] Hyman, James M., Tara Laforce, *Modeling the Spread of Influenza Among Cities*, Los Almost National Laboratory, May 2003.
- [8] Kermack, W. O., McKendrick, A. G., *A contribution to the mathematical theory of epidemics*, Proc. R. Soc., A115:700-21, 1927.
- [9] Kreysig, Erwin, *Advanced Engineering Mathematics*, 8th ed., John Wiley & Sons Inc.: USA, 1999, pp. 376-379, 920-924.
- [10] Longini, R. M., L. A. Rvachev, *A Mathematical-Model for the Global Spread OF Influenza*, Mathmatical Biosciences, 75(1):1, 1985.
- [11] Moore, Christopher, M. E. J. Newman, *Epidemics and Percolation in Small-World Networks*. Phys. Rev. E, 61:5678-5682, 2000
- [12] Newman, M. E. J., *Models of the Small World A Review*, J. Stat. Phys., 101:819-841, 2000.
- [13] Stilianakis, N. I., A. S. Perelson, and F. G. Hayden, *Emergence of drug resistance during an influenza epidemic: Insights from a mathematical model*, Journal of Infectious Diseases, 177(4):863-873, April 1998.
- [14] Watts, Duncan J., Steven Strogatz, *Collective dynamics of 'small-world' networks*, Nature, 393:440-442, 1998.

## A Solving Linear Systems of Equations

In this appendix we will explain how to find and interpret solutions to linear systems of equations. We begin by describing methods for finding and interpreting eigenvalues and eigenvectors and then discuss the role they play in solutions to linear systems. In the final section on linearization we discuss methods and reasons for approximating nonlinear systems with linear systems.

### A.1 Eigenvalues and eigenvectors

#### A.1.1 Algebraic explanation

The eigenvalues,  $\lambda_i$ , and the eigenvectors,  $v_i$ , of a matrix  $A$  satisfy the equation

$$Av = \lambda v, \quad (31)$$

where  $v \neq 0$ . In other words, the eigenvectors are vectors that the linear transformation  $A$ , acts upon by scaling with a constant, the corresponding eigenvalue. The eigenvalues can be calculated by rewriting equation (31) as,

$$(A - \lambda I)v = 0. \quad (32)$$

Since we are looking for the nontrivial solution to this equation, the determinant of  $(A - \lambda I)$  is zero. Using this condition known as the characteristic polynomial, the eigenvalues,  $\lambda_i$  can be found. Once the eigenvalues are known, the corresponding eigenvectors can be found by plugging the eigenvalues back into equation (31) [9].

**Example** We will find the eigenvalues and eigenvectors of

$$\begin{pmatrix} 3 & 4 \\ 2 & 1 \end{pmatrix}. \quad (33)$$

To find the eigenvalues, set

$$\det \begin{pmatrix} 3 - \lambda & 4 \\ 2 & 1 - \lambda \end{pmatrix} = 0 \quad (34)$$

so the characteristic polynomial is

$$\lambda^2 - 4\lambda - 5 = 0. \quad (35)$$

Solving this polynomial for its roots gives the eigenvalues  $\lambda_1 = 5$  and  $\lambda_2 = -1$ . By plugging the eigenvalues into

$$\begin{pmatrix} 3 - \lambda & 4 \\ 2 & 1 - \lambda \end{pmatrix} v_i = 0, \quad (36)$$

the two corresponding eigenvectors are found to be

$$v_1 = \begin{pmatrix} 2c_1 \\ c_1 \end{pmatrix} \text{ and } v_2 = \begin{pmatrix} c_2 \\ -c_2 \end{pmatrix}, \quad (37)$$

where  $c_1$  and  $c_2$  are constants.

### A.1.2 Geometric explanation

The matrix  $A$  may be thought of as a linear transformation which acts upon a vector. To demonstrate the geometric meaning of eigenvalues and eigenvectors we will first look at the mapping of a unit circle under the linear transformation  $A$ . Consider the two dimensional vector  $u = \begin{pmatrix} 0 \\ 1 \end{pmatrix}$ . This vector may be thought of as a point on the unit circle. Acting upon this vector with the matrix  $A = \begin{pmatrix} 4 & 1 \\ 1 & 4 \end{pmatrix}$ , gives

$$\begin{pmatrix} 4 & 1 \\ 1 & 4 \end{pmatrix} \begin{pmatrix} 0 \\ 1 \end{pmatrix} = \begin{pmatrix} 1 \\ 4 \end{pmatrix}.$$

If the vector  $u$  is thought of as a point on a plane, this says that the matrix  $A$  maps the point (0,1) to the point (1,4). Similarly, the point (1,0) would be mapped to the point (4,1). Continuing this process would reveal that the unit circle is stretched into an ellipse under the transformation  $A$ . This mapping can be characterized by the eigenvectors and eigenvalues. Using the methods described in the previous section, the eigenvalues and corresponding eigenvectors are

$$\lambda_1 = 5, v_1 = \begin{pmatrix} 1 \\ 1 \end{pmatrix} \quad \text{and} \quad \lambda_2 = 3, v_2 = \begin{pmatrix} 1 \\ -1 \end{pmatrix}.$$

The eigenvectors give the *principle directions* in which the circle is stretched and the corresponding eigenvalues tell you how much it is stretched in those directions [9]. The point (1,1) on the circle is mapped to (5,5), and the point (1,-1) is mapped to (3,-3) under  $A$ .

### A.1.3 Solving a linear system

Next we will look at the solutions to the linear system of ordinary differential equations.

$$y' = Ay, \tag{38}$$

with the initial condition  $y_0 = y(0) = x_i$ . From (38) we get

$$y'(0) = Ay(0). \tag{39}$$

It follows from the initial condition that

$$y'(0) = x'_i, \tag{40}$$

and therefore

$$Ay(0) = x'_i = Ax_i.$$

Since  $x_i$  is a solution to the system, it can be expressed as a linear combination of vectors that span the solution space, the eigenvectors  $v_i$ . That is  $y_0 = c_1 v_1 + c_2 v_2 + \dots + c_n v_n$ ,  $c_1, c_2, \dots, c_n$  constants. Thus we can write  $x'_i = Ax_i$  as

$$\sum_{i=1}^n c_i v'_i = \sum_{i=1}^n c_i A v_i,$$

from which we get

$$v_i' = Av_i. \quad (41)$$

Since the eigenvectors and eigenvalues satisfy the equation

$$Av_i = \lambda_i v_i, \quad (42)$$

(41) becomes

$$v_i' = \lambda_i v_i.$$

Since the solution to (38) will be of the form

$$y = y_0 e^{At}, \quad (43)$$

where  $e^{At} = \sum_{i=0}^{\infty} \frac{1}{i!} (At)^i$ . If we assume that  $A$  is diagonalizable, then (43) is equivalent to

$$y = y_0 e^{\lambda_i t}.$$

Substituting for  $y_0$  gives

$$y = \sum_{i=1}^n c_i v_i e^{\lambda_i t}.$$

Finally, taking the derivative gives us

$$y' = \sum_{i=1}^n \lambda_i c_i v_i e^{\lambda_i t}.$$

From this expression, we can see that the largest eigenvalue will dominate the behavior and therefore determine the growth rate. The corresponding eigenvector indicates the direction in which growth occurs.

## A.2 Linearization

Linearizing a nonlinear function or system means approximating it with a linear model while considering small perturbations. One of two main purposes for linearization is to produce linear approximations at sampled points along a solution curve which may then be interpolated to reconstruct the original curve. The other main purpose for linearization in the context of dynamical systems is to understand local behavior of nonlinear systems. This will be our focus. Because linear functions and systems of differential equations are readily analyzed and in general easier to understand than nonlinear systems, linearization is used to approximate information about the dynamics of nonlinear equations or systems of equations. By this method, linear behavior is simulated locally near a point and then results about the general domain are extrapolated based on knowledge of the nonlinear behavior.

Although many methods of linearizing exist, a widely used method is by Taylor expansion. We take the Taylor expansion around a solution to the function or system

and drop the terms of order two and higher. The expansion of the differential equation  $f(x) = x'$  around a point  $x_0$  is done as follows [3].

Let  $\delta(t) = x(t) - x_0$  be a small perturbation of  $x_0$ . We substitute into the differential equation and find

$$\delta'(t) = f(x_0 + \delta(t)).$$

Assuming the function is continuously differentiable, we take the Taylor expansion and get

$$\delta'(t) = f(x_0) + f'(x_0)\delta(t) + \frac{f''(x_0)}{2!}\delta(t)^2 + \dots + \frac{f^{(n)}(x_0)}{n!}\delta(t)^n + \dots.$$

We neglect the terms of order two and higher to get the linear model

$$\delta'(t) = f(x_0) + f'(x_0)\delta(t).$$

Linearization is often done near equilibrium points because the dynamics of the linear function near this point resemble those of the nonlinear function being approximated [3]. If  $x_0$  is an equilibrium point ( $x_0 = x_\infty$ ), then we know that

$$f(x_\infty) = 0.$$

Therefore, we get the following equation for the linear approximation near an equilibrium point,

$$v'(t) = f'(x_\infty)v(t).$$

Similarly, for a system of nonlinear ordinary differential equations,  $F(x)$ , the linearization is

$$F(x_0 + \delta(t)) = F(x_0) + D_n F(x_0)\delta(t).$$

where  $D_n F$  is the Jacobian matrix of the system. When  $x_0$  represents a solution to the system of ODE's, the Jacobian matrix gives information about how solutions changes if  $x_0$  at that point is changed. Near an equilibrium point, as before, we know that

$$F(x_\infty) = 0,$$

and we get the following system as a linear approximation near an equilibrium point,

$$V'(t) = D_n F(x_\infty)V(t).$$

Since this linear model behaves the same as the original system near an equilibrium point, the solutions may be used to determine what happens nearby in the nonlinear case. Analyzing these solutions gives eigenvectors and eigenvalues which may be used to determine the stability of the equilibria.

In this project we linearize our multipopulation SIR model near the disease free equilibrium ( $I_i = 0, i = 1..n$ ) and look at the eigenvalue and eigenvector solutions to this linearization. We evaluate the effects of network topology on these solutions to determine the effects on the initial rate of growth of the infection.